Earth Planets Space, **65**, 505–515, 2013

Volume change of the magma reservoir relating to the 2011 Kirishima Shinmoe-dake eruption—Charging, discharging and recharging process inferred from GPS measurements

Shigeru Nakao[1], Yuichi Morita[2], Hiroshi Yakiwara[3], Jun Oikawa[2], Hideki Ueda[4], Hiroaki Takahashi[5], Yusaku Ohta[6], Takeshi Matsushima[7], and Masato Iguchi[8]

[1]*Graduate School of Science and Engineering, Kagoshima University, 1-21-35 Korimoto, Kagoshima 890-0065, Japan*
[2]*Earthquake Research Institute, University of Tokyo, 1-1-1 Yayoi, Bunkyo-ku, Tokyo 113-0032, Japan*
[3]*Nansei-Toko Observatory of Earthquake and Volcano, Kagoshima University, 10861 Yoshinocho, Kagoshima 892-0871, Japan*
[4]*National Research Institute for Earth Science and Disaster Prevention, 3-1 Tenoudai, Tsukuba 305-006, Japan*
[5]*Graduate School of Science, Hokkaido University, Kita-10-jyo Nishi-8-chome, Kitaku, Sapporo 060-0810, Japan*
[6]*Graduate School of Science, Tohoku University, 6-6 Aramaki aza Aoba, Aobaku, Sendai 980-8578, Japan*
[7]*Faculty of Sciences, Kyushu University, 2-5643-29 Shinyama, Shimabara 855-0843, Japan*
[8]*Disaster Prevention Research Institute, Kyoto University, 1722-19 Sakurajima, Yokoyamacho, Kagoshima 891-1419, Japan*

(Received November 20, 2012; Revised May 28, 2013; Accepted May 29, 2013; Online published July 8, 2013)

Using GPS data, we evaluate the volume change of the magma reservoir associated with the eruption of Kirishima Shinmoe-dake volcano, southern Kyushu, Japan, in 2011. Because ground deformation around Shinmoe-dake volcano is strongly affected not only by regional tectonic movement but also by inflation of Sakurajima volcano located approximately 30–40 km to the southwest, we first eliminate these unwanted contributions from the observed data to extract the signals from Shinmoe-dake volcano. Then, we estimate the source locations and volume change before, during, and after the highest eruptive activity occurring between January 26 and 31. Our model shows that the magma began to accumulate about one year prior to the sub-Plinian eruption, with approximately 65% of the accumulated magma being discharged during the peak of the eruptive activity, and that magma accumulation continued until the end of November 2011. An error analysis shows that the sources during the three periods indicated above are located in almost the same position: 5 km to the northwest of the summit at a depth of 8 km. The 95% confidence interval of the estimated source depth is from 7.5 to 13.7 km.
Key words: Magma reservoir, GPS observation, ground deformation, the 2011 Kirishima Shinmoe-dake eruption.

1. Introduction

Shinmoe-dake volcano is a part of the Kirishima volcano group located in southern Kyushu, Japan, and is one of the most active volcanoes in the group. Prior to the 2011 eruption, phreatic explosions occurred in August 2008, and March, April, May, June, and July, 2010. A series of magmatic eruptions started on January 19, 2011, with a phreatomagmatic eruption with a trace of juvenile magma (Suzuki *et al*., 2013b). This was the first major eruption since the 1716–1717 eruption that evolved from a phreatic to a magmatic eruption (Imura and Kobayashi, 1991). A sub-Plinian eruption started in the afternoon of January 26, 2011 (local time), and two other sub-Plinian eruptions occurred, one at midnight and one in the afternoon of January 27. After the eruptions, lava started to be extruded through the conduit, and accumulated inside the summit crater between January 29 and January 31. Tiltmeters installed around the volcano showed that significant ground deflation started on January 26 and ended on 31 (Japan Meteorological Agency: JMA, 2011). The activity was most explosive during these six days, and we define this activity as the "climax event" in this paper. Vulcanian eruptions followed the climax event and lasted until September 2011. A detailed chronology of the eruptions is given by Nakada *et al*. (2013).

The volcano edifice started to inflate about a year prior to the climax event (GSI, 2011). At the same time, seismicity around the Kirishima volcano group increased and was maintained at an elevated level (JMA, 2011). To monitor the magma accumulation process, we installed GPS sites before the climax event, and added some sites after the event. In this paper, we infer the volume change of the magma reservoir associated with the 2011 Kirishima Shinmoe-dake eruption from GPS data. We processed all available dual-frequency GPS data around Shinmoe-dake volcano and detected the inflation and deflation processes before, during and after the climax event. Details of the data processing are shown in Section 2. To extract precisely the volcanic deformation which originated from Shinmoe-dake, we needed to pay close attention to the ground deformation of tectonic origin and that which originated from a nearby volcano, details of which will be described in Section 3. In Section 4, we estimate the source location and the volume change as well as their uncertainties before, during,

doi:10.5047/eps.2013.05.017

Table 1. GPS sites used in this study.

Station name	Location (latitude, longitude, altitude)			Available data
950485*[1]	32.05750	130.59782	215.733	Whole period
960714*[1]	32.04772	130.86563	287.376	Whole period
950486*[1]	31.85553	130.75967	254.584	Whole period
021087*[1]	31.87780	130.97694	400.700	Whole period
021089*[1]	31.74378	130.73569	54.561	Whole period
970837*[1]	31.82406	130.59959	314.664	Whole period
950481*[1]	31.96505	131.07857	215.905	Whole period
109078*[1]	31.99280	130.81976	519.566	after February 3, 2011
KRMV*[2]	31.93004	130.81007	971.709	after April 9, 2010
KRHV*[2]	31.92970	130.93938	694.518	after April 10, 2010
KVO*[3]	31.94731	130.83908	1229.858	after June 21. 2007
KKCD*[3]	31.98165	130.90240	539.282	after October 6, 2010
YMNK*[3]	31.95613	130.95296	335.800	after March 2, 2007
KRSP*[3]	31.84888	130.86256	394.107	after April 20, 2007
YOSG*[3]	32.01019	130.76512	363.642	after August 15, 2010
KRNO*[3]	31.95298	130.72569	228.128	after January 31, 2011
KRYK*[3]	31.94047	130.77867	753.644	after February 8, 2011
MNZS*[3]	31.90185	130.74884	224.703	after January 29, 2011
TKCH*[3]	31.88531	130.81902	553.972	after January 31, 2011

*[1]Stations operated by GSI.

*[2]Stations operated by NIED.

*[3]Stations operated by universities.

and after the climax event using the GPS data corrected using the method described in Section 3. Then we compare the model estimated in this study with geological insights and petrological analyses of melt inclusion of the lava and ash emitted during the climax event.

2. Observations and Data Analysis

In southern Kyushu, GSI installed dual-frequency GNSS receivers as a part of a nationwide GNSS network (GEONET) (e.g., Sagiya, 2004) with an average spacing of around 20 km, which provides RINEX formatted data to researchers online. Because most of the stations were constructed prior to 2002, we can analyze long-term ground deformation in relation to volcanic activity in southern Kyushu. In addition, the National Research Institute for Earth Science and Disaster Prevention (NIED) constructed two GPS stations at points several kilometers away from the summit of Shinmoe-dake volcano in 2010. Furthermore, researchers at various universities installed five GPS stations around the volcano before the eruption and added six stations after the climax event. At all the stations mentioned above, dual-frequency phase data are recorded continuously at a sampling interval of 30 seconds. The locations of these GPS stations are shown in Fig. 1 and Table 1.

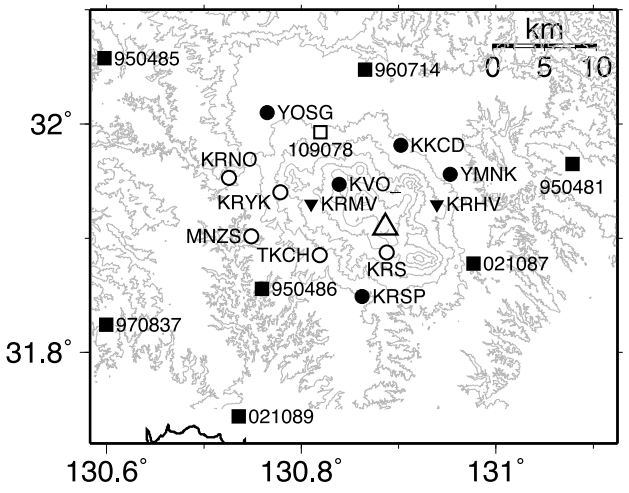

Fig. 1. Distribution of continuous GPS sites used in this study. Solid and open symbols represent stations installed before and after the climax eruption, respectively. Circles, inverse triangles and squares indicate that the stations are operated by universities, NIED, and GSI, respectively. The large open triangle shows the location of the summit of Shinmoe-dake volcano.

We combined all available dual-frequency GPS data surrounding Shinmoe-dake volcano, and estimated the daily positions of each station using Bernese GPS Software Ver. 5.0 with the Bernese Processing Engine (Dach *et al*., 2007). We used the International GNSS Service for Geodynamics (IGS) precise ephemerides and the International Earth Rotation and Reference Systems Service (IERS) Earth rotation parameters (Altamimi *et al*., 2011). The coordinates of the GPS sites were estimated with respect to ITRF2008 (Altamimi *et al*., 2011). We also estimated tropospheric delays every hour and their horizontal gradients every six hours to improve the accuracies of the station coordinates. The correction of tropospheric delay is important because rainfalls are abundant and humidity is high in the area from June to the first half of August. We used the mapping function by Boehm *et al*. (2006), which is based on a numerical weather model.

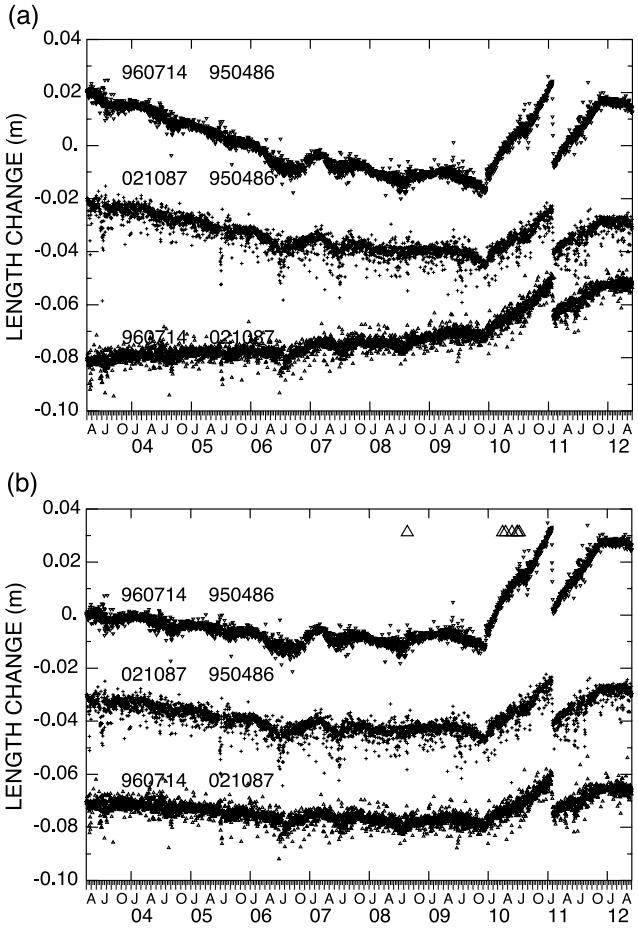

Fig. 2. An example of baseline changes of GEONET station pairs around the Kirishima volcano group. (a) Plots using raw data. (b) Plots using corrected data. Triangles in (b) indicate the time when phreatic eruptions occurred. See Section 3 for details.

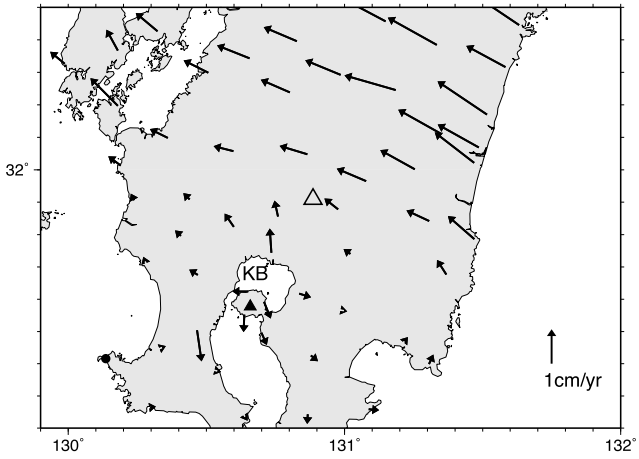

Fig. 3. The velocity field in southern Kyushu measured by GEONET with respect to a site shown as a solid circle (31.416N, 130.136E). The open triangle indicates the location of Shinmoe-dake volcano. It is clear that ground deformation around the volcano is affected by the regional tectonic deformation and dilatation due to Sakurajima volcano (small solid triangle). To estimate the ground deformation originated from Shinmoe-dake volcano, it is important to remove these deformations.

3. Removing the Effects of Tectonic Ground Deformation and the Influence of Sakurajima Volcano around Shinmoe-dake Volcano from GPS Measurements

Before we analyze the ground deformation caused by the volcanic activity at Shinmoe-dake volcano, we need to pay attention to the regional deformation in southern Kyushu, because many previous studies have suggested a complicated ground-deformation field near Shinmoe-dake volcano. Figure 2(a) shows an example of the temporal variation of the baseline lengths of three pairs of studies around Shinmoe-dake volcano (Fig. 1). All three baseline lengths began to increase simultaneously at the end of December 2009, decrease suddenly in January 2011, and then increase again until November 2011. We can confidently conclude from the spatial pattern of displacement vectors that these are caused by ground inflation and deflation beneath Shinmoe-dake volcano. In addition, linear trends in the baseline lengths are found between 2003 and 2009 (Fig. 2(a)), and such trends are larger than the inflation observed between December 2009 and January 2011. The polarity of the trends (compression or extension) is not consistent among the traces. Hence, these changes originated from the regional tectonic motions and should be eliminated before starting volcanological analysis.

The mechanisms of the regional crustal deformation in southern Kyushu are controversial. Nishimura *et al.* (2004) proposed that block rotation of the Ryukyu arc is the main factor. Takayama and Yoshida (2007) suggested that temporal variations in the inter-plate coupling affect the deformation rate. Wallace *et al.* (2009) tried to explain the deformation field assuming an east-west striking shear zone in southern Kyushu. All of these studies mentioned two common features: (1) Ground deformation in southern Kyushu is strongly affected by the subduction of the Philippine Sea Plate. However, the deformation rate is almost uniform in the southernmost Kyushu regions, but is non-uniform to the north of 32.0N, possibly reflecting the non-uniform interplate coupling. (2) Dilatational deformation is dominant around Sakurajima volcano, a very active volcano. Because the scope of this paper is to estimate ground inflation and deflation caused by magma emplacement associated with the 2011 Shinmoe-dake eruption, we simply remove these components and do not discuss deformation of a tectonic origin.

Figure 3 shows the velocity field measured by continuous GPS observations with respect to Station 960777 (solid circle in Fig. 3) over the period from November 2004 to November 2009. No significant deformation of volcanic origin occurred around Shinmoe-dake (open triangle in Fig. 3) during this period. The northwestward motion is dominant to the north of Shinmoe-dake. On the other hand, outward motions are dominant around Kagoshima Bay (that is Aira Caldera, shown as "KB" in the figure), located to the north of Sakurajima volcano (indicated by a small solid triangle). To extract the ground deformation associated with the 2011 eruption of Shinmoe-dake volcano, it is crucial to isolate that component from the overall deformation data. Here, we suppose that the observed ground displacement at the i-th station, $\mathbf{U}^i$, is composed of four components as follows:

$$\mathbf{U}^i = \mathbf{U}^i_{\text{Shinmoe}} + \mathbf{U}^i_{\text{tectonic}} + \mathbf{U}^i_{\text{Sakurajima}} + \mathbf{e}^i, \qquad (1)$$

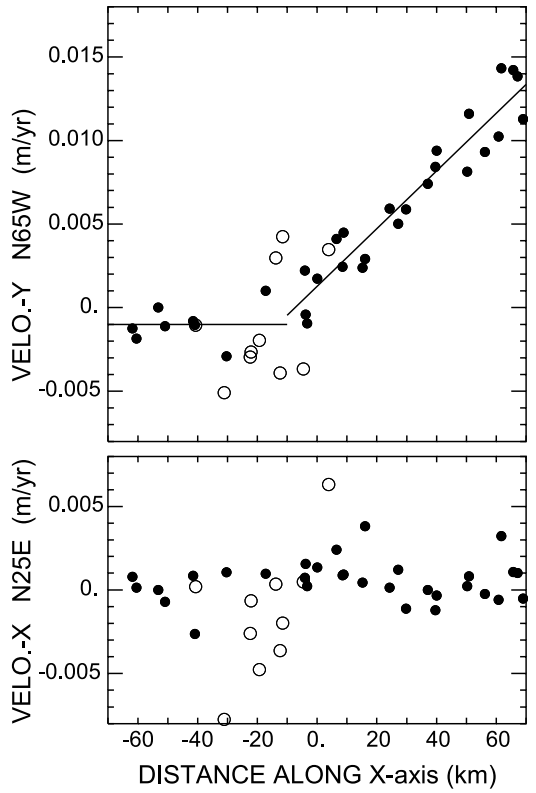

Fig. 4. Deformation velocities as a function of the distance along the x-axis (N25E direction). The top panel shows the y-component of the velocities (N65W direction), and the bottom panel shows the x-component of the velocities. The velocities of the stations close to Sakurajima volcano are plotted as open circles.

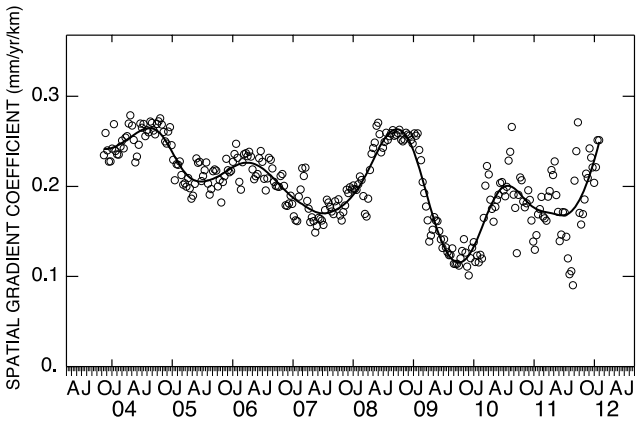

Fig. 5. Temporal variation of the coefficient of spatial gradient of northwestward deformation (a in Eq. (2)). The values are estimated every 10 days over one year, and are smoothed under the assumption that the coefficient does not change too rapidly.

where $\mathbf{U}^i_{\text{Shinmoe}}$ represents a ground displacement vector relating to the volcanic activity at Shinmoe-dake volcano, and $\mathbf{U}^i_{\text{tectonic}}$ is the tectonic ground displacement due to non-uniform interplate coupling at the Nankai Trough and the Ryukyu Trench. $\mathbf{U}^i_{\text{Sakurajima}}$ is the displacement caused by the magma accumulation beneath Sakurajima volcano, 30–40 km to the southwest of Shinmoe-dake volcano. $\mathbf{e}^i$ represents the residual. We estimate $\mathbf{U}^i_{\text{tectonic}}$ and $\mathbf{U}^i_{\text{Sakurajima}}$ from the model proposed below.

Figure 3 shows that northwestward motion dominates to the north of Shinmoe-dake, with increasing velocity toward the north. We attempted to model the northwestward velocity in the area shown in Fig. 3 as a function of station location using the following procedure. We first took the origin as 32.0N, 130.0E, and looked for the direction along which the average velocity component was largest. We found the optimum direction to be N65W, and took the x- and y-axes in the N25E and N65W directions, respectively. The upper diagram in Fig. 4 plots the y-component of the ground velocity for each station as a function of distance along the x-axis, and the lower diagram plots the x-component. Open circles represent velocities for stations around Sakurajima volcano, where the dilatational deformation are dominant. Figure 4 shows that, except for stations close to Sakurajima volcano, the y-component of ground velocity increases linearly with an increase in x in the region $x > -10.0$ km, and it is represented as follows:

$$\dot{U}^i_{x\,\text{tectonic}} = 0, \quad \dot{U}^i_{y\,\text{tectonic}} = ax^i, \quad x^i > -10\,\text{km}, \quad (2)$$

where $\dot{U}^i_{x\,\text{tectonic}}$ and $\dot{U}^i_{y\,\text{tectonic}}$ are the x- and y-components of the ground velocities at the i-th station, respectively. a is a constant defined as the coefficient of spatial gradient, x^i is the x-coordinate of the i-th station. We found that $a = 0.17$ mm/yr/km fits the observation best between November 2004 and November 2009. Here, we assumed that the ground velocity due to the tectonic deformation varies along the N25E direction and does not vary in the direction perpendicular to it. Despite the simplicity, this model fits the observation very well, with an average error of approximately 1.0 mm/yr. A similar relation has been presented by Takayama and Yoshida (2007). Our model is an advanced version of their model with modifications of the fixed point and the optimum direction.

So far we have assumed that tectonic deformation does not vary temporally. However, it actually varies over time in this region. For example, GSI (2012) reported a slow slip event (SSE) at the west coast of northern Kyushu between October in 2009 and October in 2010 with an equivalent moment magnitude of M_w 7.0, during which time the coupling was weakened and the northwestward deformation was decelerated. In order to take account of temporal variation in tectonic deformation, we estimated a in Eq. (2) as a function of time. We first calculated a over one-year periods every 10 days, and these values were smoothed under the assumption that a does not change too rapidly (Fig. 5). The estimated value of a is low on average during the period from the second half of 2009 to the first half of 2010. The value of a varies by a factor of two from time to time.

In a next step, we analyzed the dilatational deformation generated by Sakurajima volcano ($\mathbf{U}^i_{\text{Sakurajima}}$). Following a previous study (Hidayati *et al.*, 2007), we assumed two isotropic point sources (Mogi, 1958) and estimated their locations by the simulated annealing inversion method (Kirkpatrick *et al.*, 1983) using data from GEONET stations located close to Sakurajima volcano. Because the number of stations used here is small, the source depths cannot be constrained well. We fixed the depths of the two sources as 4 km and 10 km, and estimated only the horizontal locations of the sources. We also examined the model with sources

Table 2. Assumed volume sources associated with the deformation of the Sakurajima volcano.

Source type	Location (latitude, longitude, depth)		
(beneath Minami-dake, Sakurajima)			
Isotropic volume source	31.605	130.658	4.0
(beneath the Aira caldera)			
Isotropic volume source	31.675	130.720	10.0

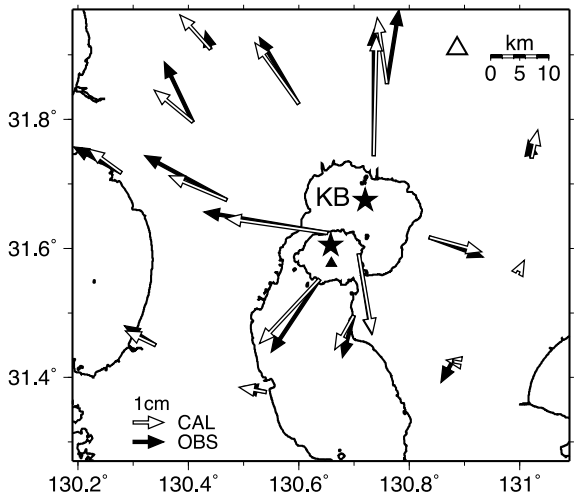

Fig. 6. Estimated location of the pressure sources beneath Sakurajima volcano. The observed and calculated horizontal displacements measured by GEONET from April 2003 to April 2009 are shown as solid and open arrows, respectively.

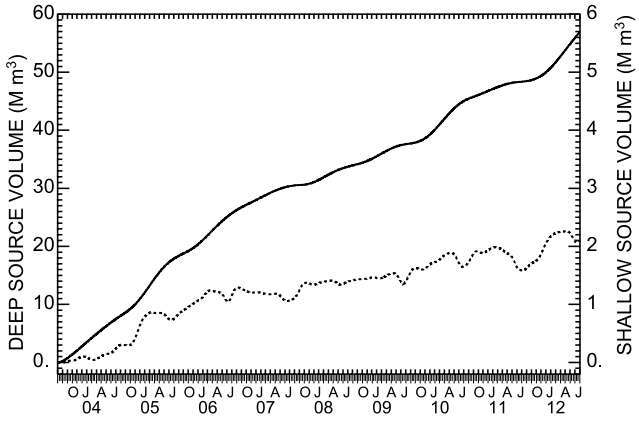

Fig. 7. The volume change of the two magma reservoirs shown in Fig. 6. The solid curve indicates the volume change of the magma reservoir located beneath Aira caldera (Kagoshima Bay; KB in Fig. 6) at a depth of 10 km during July 2003 and June 2012. The scale is shown on the left vertical axis. The broken curve shows the volume change of the reservoir beneath Sakurajima volcano at a depth of 4 km. The scale is shown on the right vertical axis.

at depths of 5 km and 10 km as proposed by Hidayati *et al*. (2007); however, the residuals increased. Figure 6 and Table 2 show the estimated locations of the two sources. Given the source locations, we evaluated the temporal volume changes of the two sources using the time-dependent inversion method (Segall and Mathews, 1997) under the assumption that the two sources do not change their positions throughout the period. Figure 7 shows the temporal volume changes of both sources, indicating that the magma beneath Aira caldera (solid curve) accumulated more rapidly between 2003 and 2006, than after 2007. Figure 2(a) shows a change in the trend in the middle of 2006, corresponding to decelerated magma accumulation beneath Aira caldera after the middle of 2006.

To extract the deformation originated from Shinmoe-dake, we removed the contribution of tectonic displacement ($\mathbf{U}_{\text{tectonic}}$) and displacement due to the dilatational source of Sakurajima volcano ($\mathbf{U}_{\text{Sakurajima}}$) from the GPS data. Figure 2(b) shows that this was successfully carried out, and the cleaned data are ready to be used to determine the deformation caused by Shinmoe-dake volcano. Figure 8 depicts the observed and calculated deformation caused by interplate coupling and Sakurajima inflation over the one-year period of 2008 at reference site 950481 (solid circle in the figure). The observed movements (solid arrows) closely match the calculated movements (open arrows) at stations relatively distant from Shinmoe-dake. This demonstrates that the ground deformation due to interplate coupling and the inflation of Sakurajima volcano are dominant there and

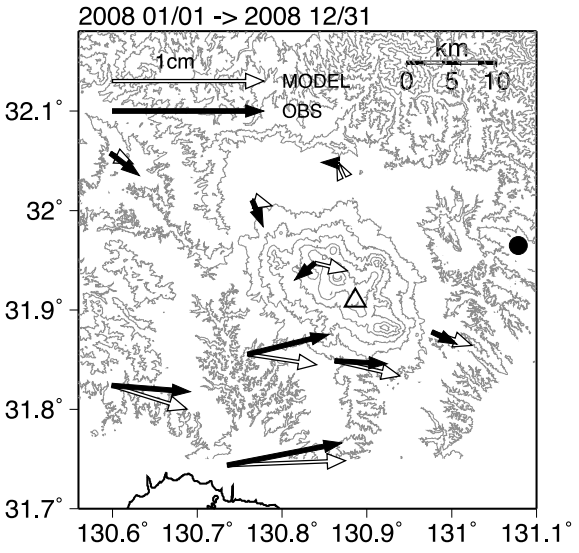

Fig. 8. Calculated (solid arrows) and observed (open arrows) ground displacements during 2008. The scale is shown in the upper left of the figure. The calculated deformation is based on a model of tectonic deformation and inflation of Sakurajima volcano. Reference station 950481 is marked with a circle.

that the model proposed here well reproduces their contributions. During the volcanic activity at Shinmoe-dake (from November 2009 to November 2011), the deformation caused by these two factors is approximately two-thirds of the average rate between 2003 and 2009. The reduced rate of the deformation stems from the weakened interplate cou-

Table 3. Optimum location with 95% confidence intervals of the pressure source for the period before, during and after the climax event.

Period	Latitude (deg.)	Longitude (deg.)	Depth (km)	Volume (10^6 m^3)
(Inflation process before the climax event)				
2010 Aug. 20–	31.932N	130.830E	9.18	7.92
2011 Jan. 25	(31.923–31.940)	(130.814–130.845)	(7.49–13.66)	(5.80–14.49)
(Deflation process during the climax event)				
2011 Jan. 15–	31.942N	130.831E	8.35	−13.35
2011 Feb. 11	(31.934–31.946)	(130.825–130.840)	(7.36–10.84)	(−10.42–−17.69)
(Inflation process after the climax event)				
2011 Feb. 25–	31.937N	130.829E	8.18	10.17
2011 Nov. 25	(31.926–31.942)	(130.824–130.842)	(7.09–9.88)	(7.96–13.82)

pling (Fig. 5) and the slow inflation of Sakurajima volcano (Fig. 7). The ground deformation caused by these two factors during the period would be smaller than the example shown in Fig. 8. Nevertheless, we emphasize that we need to remove these unwanted displacement components.

4. Volume Change of the Magma Reservoir beneath Shinmoe-dake Volcano

From the temporal changes of the corrected baseline shown in Fig. 2(b), we can infer the entire process of accumulation and discharge of magma related to the 2011 Kirishima Shinmoe-dake eruption. Here, we use the GPS data corrected using the model mentioned in the previous section. The volcano inflated slowly before the climax event, it deflated rapidly during the climax event, and then inflated again after the event. In this study, we divide the period of activity into three parts: (1) inflation period prior to the climax event, from the beginning of inflation (the end of December 2009) to just before the sub-Plinian eruption (January 25, 2011); (2) the deflation period during the climax event, from the beginning of the sub-Plinian eruption (January 26, 2011) to the time when magma extrusion to the summit crater terminated (January 31, 2011); and (3) the secondary inflation period after the climax event, from February 1 to the end of November when the inflation stopped. We estimated the source location and volume change during the three periods, independently.

We model the deformation field assuming a single isotropic source, or the Mogi source (Mogi, 1958), embedded in an elastic, isotropic, and homogenous half space. These assumptions might be too simple and unrealistic. For example, the subsurface structure is layered, and the magma reservoir is not a point. Nevertheless, considering the limited number of stations, we did not introduce a complex source model and realistic underground structure.

We calculated the temporal evolution of three-dimensional ground deformation by computing averages over the first 10 days and the last 10 days of the time window, and subtracted the latter from the former. We defined the uncertainty as a standard deviation of the estimated positions. The time windows were selected so that the number of available stations was maximized, because the GPS data were sometimes lost due to electric power failures at the sites. We also checked the quality of the data within the specified time window. Finally, we selected the periods listed in Table 3. Using the simulated annealing inversion method (Kirkpatrick *et al.*, 1983), we estimated the source location and volume change for the three periods. We weighted the data according to the uncertainties, which were 1 mm or less for the horizontal components and 3–5 mm for the vertical component. We took the differential displacement for all the station pairs to eliminate the effect of uniform deformation over the whole network. Because the tectonic deformation and the inflation generated by Sakurajima volcano vary spatially (see Fig. 8), we obtained different results with different reference sites even after the data were corrected as described in the previous section.

Firstly, we show the source location after the climax event, because we can use many GPS stations to estimate it. Then, we show the source location before the climax event, for which we can use fewer GPS stations. Figures 9(a) and (b) compare the observed and calculated displacements after the climax event. The star is the location of the pressure source. The observed horizontal displacements are radial from the estimated source location and fit well with the calculations (see Fig. 9(a)). This pattern is consistent with an isotropic point source. Figure 9(b) shows that large uplifts are observed just above the source, which is also consistent with the point source model. Figures 9(c) and (d) show displacements and the source location before the climax event. There are fewer GPS stations before the climax event (Figs. 9(c) and (d)) than after the climax event (Figs. 9(a) and (b)), but their azimuthal coverage around the source is good, so the horizontal location of the source prior to the climax event was also constrained well. However, the depth was not so well constrained as the source after the climax event.

We also evaluated errors in the estimated parameters (the source location and the volume change) using the bootstrap method (e.g., Wang and Taguri, 1996). This method is often used for evaluating errors when the statistical properties of the observation errors are not well known. We calculated the residuals between the observed and calculated displacements derived from a best-fit model, and added randomly re-sampled residuals to form an artificial dataset. We then performed the same inversion using the artificial dataset. We repeated the inversion 500 times and checked the probability distribution of the estimated parameters, which represents the uncertainties and trade-offs between parameters (Wang and Taguri, 1996). Figure 10 shows the correlation between the estimated source location and volume change for the period after the climax event, exhibiting a distinct

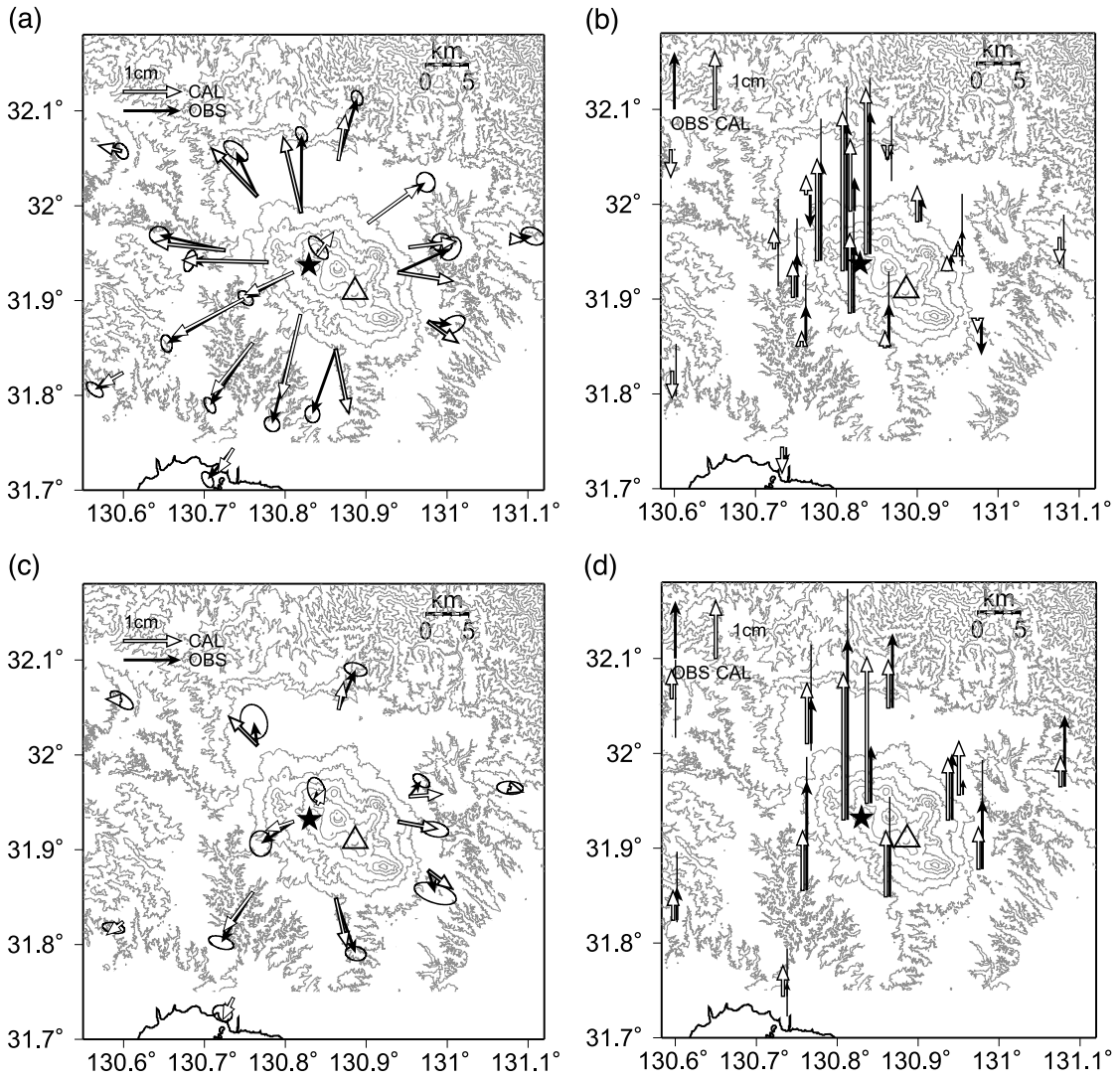

Fig. 9. (a) Observed (solid arrows) and calculated (open arrows) displacements after the climax event. The location of a spherical inflation source is depicted by a star. The ellipsoids at the tips of solid arrows indicate observation errors. The scale is shown in the upper left of the figure. (b) Vertical displacements. Thin lines show observation errors. (c) Same as (a), before the climax event. (d) Same as (b), before the climax event.

trade-off between the estimated source depth and volume change. At the same time, almost no trade-offs are seen between other parameters. We also find similar trade-offs between the source depth and volume change in the models of other periods (Fig. 11).

Figure 12 shows the distribution of the source depths derived from the bootstrap analysis, indicating that the source depth is estimated at 8–9 km as the optimum value. Figure 13 depicts the horizontal location of the sources during the three periods derived by the bootstrap analysis. All three sources are located close to each other approximately 5 km to the northwest of the Shinmoe-dake summit. The detailed source locations and volume changes are summarized in Table 3 as optimum values and their 95% confidence intervals. The addition of GPS stations after the climax event reduced uncertainties.

Accumulation and the discharge rate of magma are important parameters that control whether an eruption is explosive or effusive. Table 4 shows that the total magma accumulation before the climax event is 21×10^6 m^3 and that the accumulation rate is 0.6 m^3/s. During the climax eruption, the total volume of magma extrusion is 13×10^6 m^3 at a rate of 25.8 m^3/s, and the total accumulation after the eruption is about 11×10^6 m^3 at a rate of 0.4 m^3/s. These values are based on several assumptions such as simplified source geometry and material. Therefore, although the estimated values can safely be used for comparisons within the three periods, it is inappropriate to compare them with the actual quantity of the erupted magma without any consideration of the limitations of the assumptions used here. This will be discussed in the next section in detail. Also note that the temporal resolution of GPS data is low, and so the estimated rates of volume changes just represent temporal averages. Rapid temporal variation of the discharge rate during a climax event has been demonstrated by Kozono *et al.* (2013) using high time-resolution tilt data, but it is impossible with our GPS data.

5. Discussion

Several phreatic explosions were observed prior to the sub-Plinian eruption in January 2011, the largest of which occurred on August 22, 2008 (Geshi *et al.*, 2010). Figure

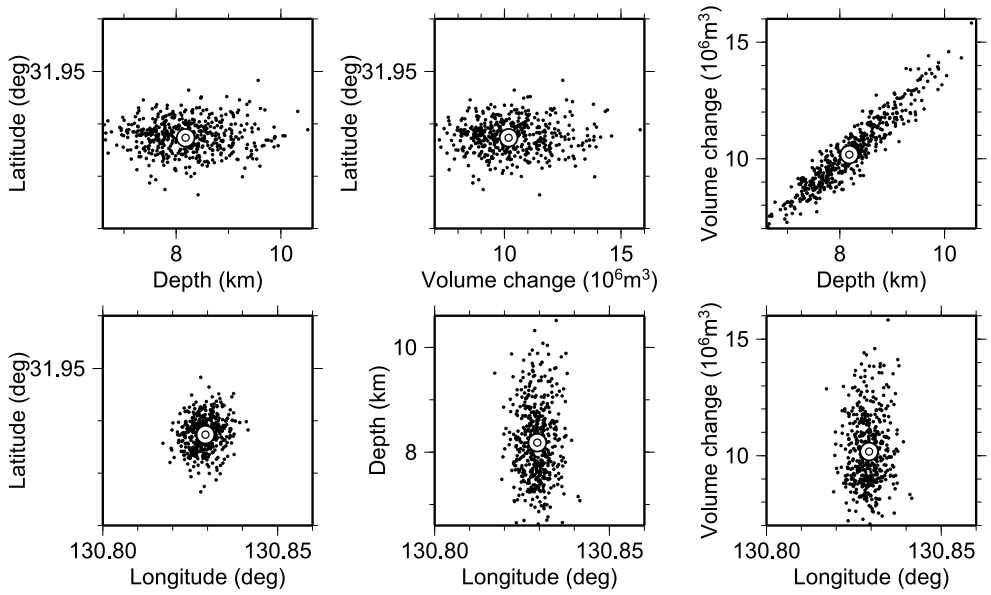

Fig. 10. Trade-offs between estimated source parameters for the period after the climax event. The open double circle shows the best fit model. Dots indicate estimates of bootstrap tests. Estimated source volume and depth have a strong trade-off, while other parameters show little correlation.

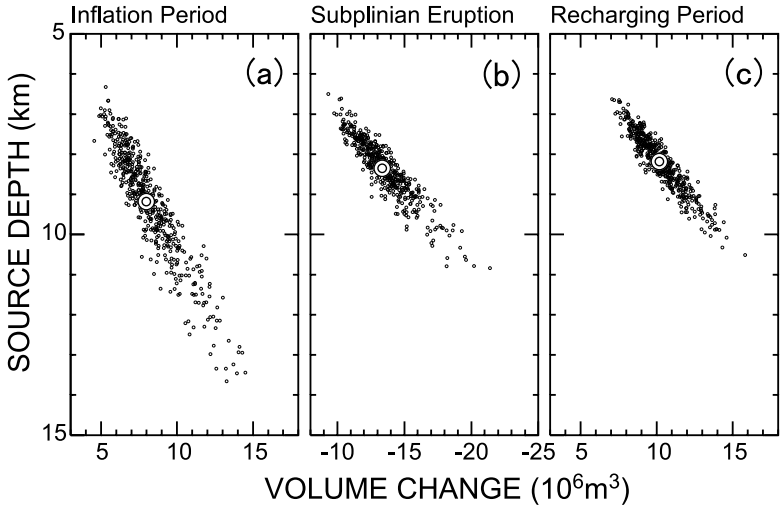

Fig. 11. Trade-offs between estimated source depth and volume change for the period before, during and after the climax event. Double open circles show the values of the optimum model and dots represent estimates of bootstrap tests.

Table 4. Estimated total volume and accumulation or discharging rate of magma for the period before, during and after the climax event and their 95% confidence intervals.

Period	Time interval (days)	Total volume (10^6 m^3)	Accumulation rate in average (m^3/s)
(Inflation process before the climax event)			
From Dec. 25, 2009	396	20.6	0.60
Till Jan. 25, 2011		(15.1–37.7)	(0.44–1.10)
(Deflation process during the climax event)			
From Jan. 26, 2011	6	13.4	25.8
Till Jan. 31, 2011		(10.42–17.69)	(20.1–34.1)
(Inflation process after the climax event)			
From Feb. 2, 2011	297	11.2	0.43
Till Nov. 25, 2011		(8.6–15.0)	(0.33–0.58)

2(b) indicates that the magma was not stored in the reservoir estimated here prior to the 2008 eruption. On the other hand, Takagi *et al.* (2011) found an inflation source localized near the summit of Shinmoe-dake between 2006 and 2008 from the data of three single-frequency continuous GPS stations (installed by JMA) within 2 km from the summit of Shinmoe-dake volcano and four campaign GPS sites on the rim of the summit crater. The source location was es-

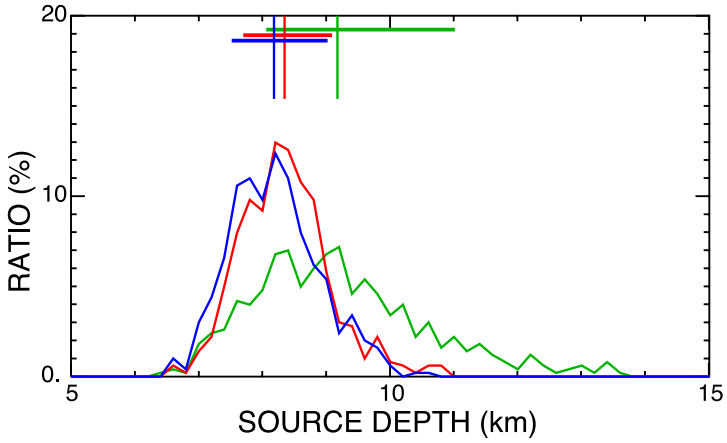

Fig. 12. Probability distribution of the estimated source depths derived from bootstrap tests. The optimum depths are shown as vertical lines with ranges of standard deviations as horizontal lines. The green, red and blue curves show the distribution of the estimated depths before, during and after the climax event, respectively.

timated as being several hundred meters beneath the summit, indicating that the pressure source at a shallow depth may also have been inflated during the 2011 eruption. However, the GPS network used in this study is sparse and cannot detect the inflation of magma sources in shallow depths close to the summit crater. Our results do not rule out the presence of shallow and small magma sources during the 2011 eruption. Joint analysis of regional GPS sites used in this study and those installed close to the summit crater is required to reveal the more detailed process of the eruption to address the behavior of the shallow source.

In this study, we assumed that the source is an isotropic point source embedded in a homogenous and elastic half-space. The real magma reservoir is not an infinitesimal sphere, and the crust has heterogeneous and layered structures. Many previous studies have tried to model ground deformation by using a complex source geometry (e.g., Hashimoto and Tada, 1988; Segall *et al.*, 2001; Ueda *et al.*, 2005), or heterogeneous crustal structures (e.g., De Natale and Pingue, 1993; Fernandez and Rundle, 1994; Trasatti *et al.*, 2003). We acknowledge that the models used in this study are too simple to represent real phenomena, the limited station distribution does not allow us to introduce a complex source model or heterogeneous crustal structure. Here, we just show how our results will change by assuming a heterogeneous crustal structure. Hautmann *et al.* (2010) estimated the effect of a realistic underground structure using a finite-element method. Their model involves a single discontinuity and a Young's modulus increasing with depth, which is more realistic than the homogeneous half-space assumed in this study. Hautmann *et al.* (2010) showed that the source depth tends to be underestimated by incorrectly assuming a uniform half-space. This reflects an enhancement of the horizontal component of surface displacement relative to the vertical component caused by the presence of a low-rigidity layer near the ground surface. However, this effect becomes minor if the source depth is greater than around 10 km. Therefore, our study may have underestimated the source depth to some extent, i.e., the source may be deeper than 8 km and volume changes may be larger. However, such differences are not serious, because the estimated source depth is deep enough.

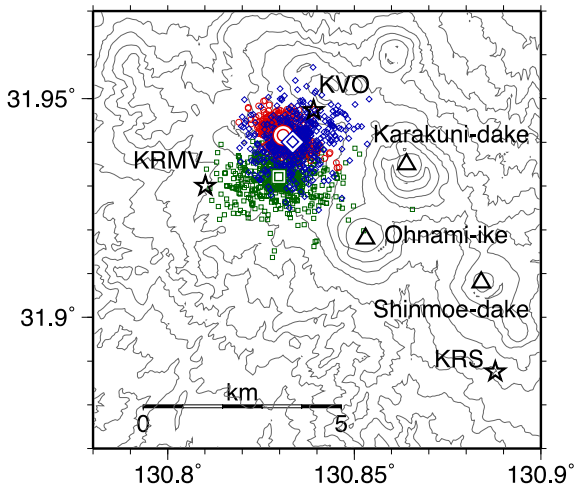

Fig. 13. Bootstrap realizations of horizontal locations of pressure sources for the period before the climax event (green rectangles), during the climax event (red circles) and after the climax event (blue diamonds). The optimum locations are plotted as large open marks. Stars are the locations of GPS sites used in this study.

Nakada *et al.* (2013) estimated the total amount of magma erupted during the climax eruption from the ejected tephra and the volume of lava accumulated in the summit crater. They concluded that the total amount was 21–27 $\times$ 10^6 m^3 DRE (dense rock equivalent). Our analysis shows that the reservoir deflated 13.4×10^6 m^3 (with the 95% confidence interval between 10.4 and 17.7 $\times$ 10^6 m^3), and this is smaller than the magma volume extruded to the surface during the climax event. The ratio of the extruded magma volume to the deflation volume (Rv) is 1.8 ± 0.5. The value is affected not only by the magma compressibility (Rivelta and Segall, 2008) but also by the shape of the magma reservoir (Amoruso and Crescentini, 2009). Rivalta and Segall (2008) pointed out that the ratio should be greater than one if the magma within the reservoir is compressible. They presented observed facts that $Rv = 3.8 \pm 0.8$ for the 1997 intrusion/eruption at Kilauea volcano, and $Rv = 5 \pm 1$ for

the 2005 dike intrusion at Afar. The value estimated here is smaller than the values mentioned above, and it may reflect the fact that the magma within the reservoir beneath Shinmoe-dake is less compressible than the above cases.

Next, we again discuss the magma source location prior to the climax event. The source depth of 9.2 km prior to the climax event is slightly deeper that those during (8.3 km) and after (8.2 km) this event. Considering the confidence intervals, it cannot be proved that the source depth became shallower after the climax event. Nevertheless, we point out the possibility that the source actually became shallower after the climax event. From petrological analyses of the melt inclusions in lava and ash ejected during the climax eruption, Suzuki *et al*. (2013a) asserted that the eruption involved two separate magma reservoirs: a silicic andesitic magma reservoir as deep as 5 km or so (125 MPa), and a basalt andesitic reservoir as deep as 10 km or so (250 MPa). They demonstrated that a small amount of basalt andesite magma at a high temperature migrated upward and partly melted the silicic andesite magma reservoir prior to the sub-Plinian eruption. This process led to a reduction in viscosity of the silicic andesite magma and gave rise to a sub-Plinian eruption. According to their model, magma accumulated mainly in the deeper part of the reservoir prior to the climax eruption. If the magma recharged in the region where both silicic magma and basalt andesite magma remained after the climax event, the source would have become shallower than the depth prior to the climax event.

6. Conclusions

To understand the relation between magma accumulation and volcanic eruption in the 2011 Kirishima Shinmoe-dake eruption, we analyzed GPS data and evaluated ground inflation and deflation quantitatively. Because the ground deformation near Shinmoe-dake volcano was strongly affected by regional tectonic deformation as well as dilatational deformation generated by Sakurajima volcano, we subtracted these effects from the GPS measurements and reduced the effects from observed GPS data to extract the signals caused by magma emplacement at Shinmoe-dake volcano.

From long-term deformation data, we saw that magma began to accumulate during a one-year period, and was then discharged rapidly over 6 days during the climax event, and was recharged during the post-eruption period of around 10 months. The edifice began to inflate at the end of November 2009 and continued until just before the sub-Plinian eruption. The charging rate was 0.6 m^3/s on average and the total amount of magma reached 21×10^6 m^3. The estimated location of the reservoir was about 5 km to the northwest of the summit crater of Shinmoe-dake volcano at a depth of 8–9 km. During the climax event, the magma reservoir shrank by 13×10^6 m^3 in volume, which is smaller than the amount of erupted magma volume estimated from geological surveys (24×10^6 m^3 DRE). This mismatch would reflect the compressible property of magma. The magma was stored again at the same place just after the climax event and the recharging process continued until the end of November. The total amount of the recharged magma was 11×10^6 m^3, with an average recharging rate of 0.4 m^3/s. Using the bootstrap method, the source location for the three periods is presented with confidence intervals.

Acknowledgments. The authors express great thanks to the anonymous reviewers and the editor whose suggestions were very helpful in improving this manuscript. They pointed out the incompleteness of our analysis. We are also greatly indebted to Prof. Kosuke Heki for improving the manuscript. We are grateful to Dr. Kazuhiko Goto, Mr. Shuichiro Hirano, Mr. Yasuhiro Hirata, and Mr. Masayoshi Ichiyanagi for helping to construct GPS stations after the sub-Plinian eruption. We are also grateful to Kirishima Primary School, Nation Livestock Breeding Center Miyzaki Station, Kita-Kirishima Cosmo Dome, Takachiho Primary School, Manzen Primary School, Kurino Primary School, and Kirishima Open-air Museum for providing us with the GPS observation sites. We express great thanks to the Geospatial Information Authority of Japan and the National Research Institute for Earth Science and Disaster Prevention for providing GPS data. We also wish to express our gratitude to Prof. S. Nakada for letting us join the research group of the 2011 Kirishima Sinmoe-dake eruption. This research was supported by MEXT/JSPS KAKENHI grant 22900001.

References

Altamimi, Z., X. Collilieux, and L. Metivier, ITRF2008: An improved solution of the international terrestrial reference frame, *J. Geod.*, **85**, 457–473, 2011.

Amoruso, A. and L. Crescentini, Shape and volume change of pressurized ellipsoidal cavities from deformation and seismic data, *J. Geophys. Res.*, **114**, B02210, doi:10.1029/2008JB005946, 2009.

Boehm, J., B. Wel, and H. Schuh, Troposphere mapping functions for GPS and very long baseline interferometry from European Centre for Medium-Rnage Weather Forecasts operational analysis data, *J. Geophys. Res.*, **111**, B02406, doi:10.1029/2005JB003629, 2006.

Dach, R., U. Hugentobler, P. Fridez, and M. Meindl, *Bernese GPS Software Version 5.0*, 612 pp., Astronomical Institute, University of Bern, 2007.

De Natale, G. and F. Pingue, Ground deformations in collapsed caldera structure, *J. Volcanol. Geotherm. Res.*, **57**, 19–38, 1993.

Fernandez, J. and J. B. Rundle, FORTRAN program to compute displacement, potential and gravity changes resulting from a magma intrusion into a gravitational layered Earth model, *Comput. Geosci.*, **20**, 461–510, 1994.

Geshi, N., S. takarada, M. Tsutsui, T. Mori, and T. Kobayashi, Products of the August 22, 2008 eruption of Shinmoedake volcano, Kirishima volcano group, Japan, *Bull. Volcanolo. Soc. Jpn.*, **55**, 53–64, 2010 (in Japanese with English abstract).

GSI (Geospatial Information Authority of Japan), Crustal deformations around Kirishima volcano, *Rep. Coord. Comm. Predict. Volcan. Erup.*, **106**, 154–161, 2011 (in Japanese).

GSI (Geospatial Information Authority of Japan), crustal movements in the Chugoku and Shikoku districts, *Rep. Coord. Comm. Earthq. Predict.*, **87**, 438–447, 2012 (in Japanese).

Hashimoto, M. and T. Tada, Crustral deformations before and after the 1986 eruption of Izu Oshima volcano, *Bull. Volcano. Soc. Jpn.*, **33**, S136–S144, 1988 (In Japanese with English abstract).

Hautmann, S., J. Gottsmann, R. S. J. Sparks, G. S. Mattioli, I. S. Sacks, and H. Strutt, Effect of mechanical heterogeneity in arc crust on volcano deformation with application to Soufriere hills Volcano, Montserrat, West Indies, *J. Geophys. Res.*, **115**, B09203, doi:10.1029/2009JB006909, 2010.

Hidayati, S., K. Ishihara, and M. Iguchi, volcano-tectonic earthquakes during the stage of magma accumulation at the Aira caldera, Southern Kyushu, Japan, *Bull. Volcano. Soc. Jpn.*, **52**, 289–309, 2007.

Imura, R. and T. Kobayashi, Eruptions of Shinmoe-dake volcano, Kirishima volcano group, in the last 300 years, *Bull. Volcano. Soc. Japan*, **36**, 135–148, 1991 (in Japanese with English abstract).

JMA (Japan Meteorological Agency), Volcanic activity of Kirishima volcano—January–May, *Rep. Coord. Comm. Predict. Volcan. Erup.*, **106**, 129–147, 2011 (in Japanese).

Kirkpatrick, S., C. D. Gelatt, and M. P. Vecchi, Optimization by simulated annealing, *Science*, **220**, 671–680, 1983.

Mogi, K., Relations of the eruptions of various volcanoes and deformation of ground surfaces around them, *Bull. Earthq. Res. Inst. Univ. Tokyo*, **36**, 94–134, 1958.

Kozono, T., H. Ueda, T. Ozawa, T. Koyaguchi, E. Fujita, A. Tomiya, and

Y. J. Suzuki, Magma discharge variations during the 2011 eruptions of Shinmoe-dake volcano, Japan, revealed by geodetic and satellite observations, *Bull. Volcanol.*, **75**, 695, doi:10.1007/s00445-013-0695-4, 2013.

Nakada, S., M. Nagai, T. Kaneko, Y. Suzuki, and F. Maeno, The outline of the 2011 eruption at Shinmoe-dake (Kirishima), Japan, *Earth Planets Space*, **65**, this issue, 475–488, doi:10.5047/eps.2013.03.016, 2013.

Nishimura, S., M. Hashimoto, and M. Ando, A rigid block rotation model for the GPS derived velocity field along the Rukyu arc, *Phys. Earth Planet. Inter.*, **142**, 185–203, 2004.

Rivalta, E. and P. Segall, Magma compressibility and the missing source for some dike intrusions, *Geophys. Res. Lett.*, **35**, L04306, doi:10.1029/2007GL032521, 2008.

Sagiya, T., A decade of GEONET: 1994–2003—The continuous GPS observation in Japan and its impact on earthquake studies—, *Earth Planets Space*, **56**, xxix–xli, 2004.

Segall, P. and M. Matthews, Time dependent inversion of geodetic data, *J. Geophys. Res.*, **102**, 22391–22409, 1997.

Segall, P., P. Cervelli, S. Owen, M. Lisowski, and A. Miklius, Constraints on dike propagation from continuous GPS measurements, *J. Geophys. Res.*, **106**, 19301–19317, 2001.

Suzuki, Y., A. Yasuda, N. Hokanishi, T. Kaneko, S. Nakada, and T. Fujii, Syneruptive deep magma transfer and shallow magma remobilization during the 2011 eruption of Shimoe-dake, Japan—Constraints from melt inclusions and phase equailibria experiments—, *J. Volcanol. Geotherm. Res.*, **257**, 184–204, 2013a.

Suzuki, Y., M. Nagai, F. Maeno, A. Yasuda, N. Hokanishi, T. Shimano, M. Ichihara, T. Kaneko, and S. Nakada, Precursory activity and evolution of the 2011 eruption of Shinmoe-dake in Kirishima volcano—insights from ash samples, *Earth Planets Space*, **65**, this issue, 591–607, doi:10.5047/eps.2013.02.004, 2013b.

Takagi, A., K. Fukui, S. Onizawa, T. Yamamoto, K. kato, S. Chikazawa, K. Fujiwara, and T. Sakai, Ground deformation around Shinmoe crater before the 2011 Kirishima eruption, *Abstract of Fall Meeting Volcanological Society of Japan*, 119, 2011 (in Japanese).

Takayama, H. and A. Yoshida, Crustal deformation in Kyushu derived from GEONET data, *J. Geophys. Res.*, **112**, B06413, doi:10.1029/2006JB004690, 2007.

Trasatti, E., C. Giunchi, ans M. Benafode, effect of topography and rheological layering on ground deformation in volcanic regions, *J. Volcanol. Geotherm. Res.*, **112**, 89–110, 2003.

Ueda, H., E. Fujita, M. Ukawa, E. Yamamoto, and M. Irwan, magma intrusion and discharge process at the initial stage of the 2000 activity of Miyakejima, central Japan, inferred from tilt and GPS data, *Geophys. J. Int.*, **161**, 891–906, 2005.

Wallace, L. M., S. Ellis, K. Miyao, S. Miura, J. Beavan, and J. Goto, Enigmatic, highly active left lateral shear zone in southwest japan explained by aseismic ridge collision, *Geology*, **37**, 143–146, 2009.

Wang, J. W. and M. Taguri, Bootstrap method—An introduction from a two sample problem, *Proc. Inst. Statistical Math.*, **44**, 3–18, 1996.

S. Nakao (e-mail: nakao@sci.kagoshima-u.ac.jp), Y. Morita, H. Yakiwara, J. Oikawa, H. Ueda, H. Takahashi, Y. Ohta, T. Matsushima, and M. Iguchi